Phys. Chem. Chem. Phys.

PERSPECTIVE

Closed Bipolar Electrochemistry in a Four-Electrode Configuration

Alonso Gamero-Quijano,[a] Andrés F. Molina-Osorio,[a] Pekka Peljo[b] and Micheál D. Scanlon[a,c]*

Received 00th January 20xx,
Accepted 00th January 20xx

DOI: 10.1039/x0xx00000x

www.rsc.org/

Closed bipolar electrochemistry in a 4-electrode configuration is a highly versatile, but under-utilized, technique with major potential to emerge as a powerful methodology impacting areas as diverse as spectro-electroanalysis, energy storage, electrocatalysis and electrodeposition. In this perspective, we provide the thermodynamic framework for understanding all such future applications of closed bipolar electrochemistry in a 4-electrode configuration. We distinguish the differences between open and closed bipolar electrochemical cells. In particular, the use of the 4-electrode configuration in both open and closed bipolar electrochemical cells with immiscible aqueous-organic solutions is outlined. A comprehensive overview of the influence of external bias on the thermodynamics underpinning electron transfer from an organic redox couple to an aqueous redox couple, or *vice versa*, by electrons flowing along a conducting bipolar electrode serving as an electronic bridge is provided. Fermi level equilibration between redox species at opposite poles of a bipolar electrode under external bias is discussed. The concept of the Line of Zero Overpotential (LZO) on the bipolar electrode at steady-state conditions under an external bias is introduced. The influence of a series of experimental variables (redox potential of each redox couple, rate constant of electron transfer at each pole, an excess bulk concentration of one redox couple over the other, and areas of the poles of the bipolar electrode in contact with each electrolyte solution) on the final position of the LZO on the bipolar electrode is highlighted. A cyclic voltammogram obtained using a closed bipolar electrochemical cell in a 4-electrode configuration with immiscible aqueous-organic electrolyte solutions is explained using the thermodynamic theory detailed throughout the perspective. The theory presented herein is equally applicable to a closed bipolar electrochemical cell in a 4-electrode configuration with aqueous electrolyte solutions, each containing redox active species, in both compartments connected by a bipolar electrode.

1. Introduction to open and closed bipolar electrochemical cells

A bipolar cell typically consists of two (or more) "driving electrodes" connected to a power source and a wireless bipolar electrode (BPE) in solution, free of any external electrical connection. External bias of the driving electrodes induces an electric field in the solution, with the potential gradient varying along the length of the BPE. The isolated BPE has a floating potential.[1] Thus, the magnitude of the interfacial potential difference between the BPE and the solution varies as a function of location across the BPE, in parallel to the driving electric field, and drives electrochemical reactions at the surface of the BPE.[2] With sufficient external bias, a significant potential difference may be established between the two ends of the BPE. This leads to poles of opposite overpotential, *i.e.*, anodic and cathodic regions, on the BPE with asymmetric Faradaic reactions (oxidation and reduction, respectively) occurring at either end.[3] The versatility of the bipolar configuration has been demonstrated by its use in a variety of fields such as spectro-electroanalysis,[4–6] energy storage,[7–9] electrocatalysis,[10–12] electrografting,[13–15] and electrodeposition.[16–18]

Bipolar electrochemistry can be carried out in two primary configurations, either with an open bipolar electrochemical cell (OBPEC) or a closed bipolar electrochemical cell (CBPEC). The BPE in an OBPEC is located in a single electrolyte solution and, on establishment of a sufficient potential difference between the two poles of the BPE, an electrochemical current is produced either as a flow of electrons along the BPE (electronic pathway) or as the movement of ions in the electrolyte solution (ionic pathway). Therefore, to maximize the flow of electrons, it is necessary to use a conductive BPE in a resistive electrolyte solution, the classic example being the body of work by Kuhn and co-workers with Janus nanoparticles in the presence of a bias over 10 V.[19] Meanwhile, in a CBPEC, the two poles of the BPE simultaneously contact two electrolyte solutions, each with one driving electrode, that are spatially separated in distinct compartments.[20,21] Thus, the electrochemical current may only pass through the BPE as a flow of electrons, with the ionic pathway being totally eliminated.[22,23] Furthermore, the CBPEC configuration provides a new level of flexibility in terms of experimental design as different electrolyte solutions with diverging chemical compositions (nature of the solvent and solute), can be implemented in the two separate compartments

[a] *The Bernal Institute and Department of Chemical Sciences, School of Natural Sciences, University of Limerick (UL), Limerick V94 T9PX, Ireland, E-mail: micheal.scanlon@ul.ie*
[b] *Research group of Physical Electrochemistry and Electrochemical Physics, Department of Chemistry and Materials Science, Aalto University, PO BOX 16100, 00076 Aalto, Finland*
[c] *Advanced Materials and Bioengineering Research (AMBER) Centre*

and subjected to distinct experimental conditions (pH, temperature, exposure to light, *etc.*). These advantages of the CBPEC configuration have seen interest spike in this topic for applications ranging from the spatial separation of hydrogen and oxygen gas produced in water electrolyzers,[7] the *in operando* investigation of electrical coupling between Photosystem 1 and Photosystem 2,[24] and the development of an electrochromic sensor for multiplex detection of metabolites.[25]

2. 4-electrode open and closed bipolar electrochemical cells with immiscible aqueous-organic electrolyte solutions

A key issue in bipolar electrochemistry is optimization of the potential applied to the driving electrodes to achieve the desired polarization of the BPE, and thereby initiate electrochemical reactions at the anodic and cathodic poles. The latter may be achieved for an OBPEC configuration by careful preliminary characterization of the redox systems involved using a conventional 3-electrode electrochemical cell.[26] However, for a CBPEC, the use of a 4-electrode configuration is optimal with each separate compartment containing both a driving electrode and a reference electrode.[20,21,27] Specifically, in one compartment the driving and reference electrodes are connected to the counter and reference terminals, respectively, of the potentiostat, while in the other compartment the driving and reference electrodes are connected to the working and sensing terminals, respectively.

The 4-electrode configuration has been successfully employed to achieve bipolar electrochemistry using immiscible aqueous-organic electrolyte solutions both in an OBPEC configuration and in a CBPEC configuration (Scheme 1). A unique feature of using immiscible aqueous-organic solutions is the requirement to use an "organic reference solution" to stabilize the organic reference electrode and eliminate potential shifts (Scheme 1).[28] The latter involves immersing a metallic Ag/AgCl electrode in an aqueous solution of chloride. This aqueous chloride solution contacts the organic phase and must have a counter-ion that is the same as the cation in the organic phase. The common cation partitions at the interface formed between the organic reference solution and organic phase, known as the reference interface, equilibrates and sets up an interfacial potential difference. Therefore, during a potentiodynamic experiment (cyclic voltammetry for example), the potential applied between the two reference electrodes is the sum of two contributions, the Galvani potential difference between the two phases ($\Delta_o^w \phi$), and the potential difference between the organic reference solution and the organic phase.[28]

In the OBPEC configuration, the "wireless BPE" takes the form of conductive catalytic nanoparticles (NPs) or microparticles floating at the immiscible aqueous-organic interface in a 4-electrode electrochemical cell originally designed for electrochemistry at the interface between two immiscible electrolyte solutions (ITIES).[29] Effectively, these conductive floating BPEs facilitate catalysis *via* direct interfacial

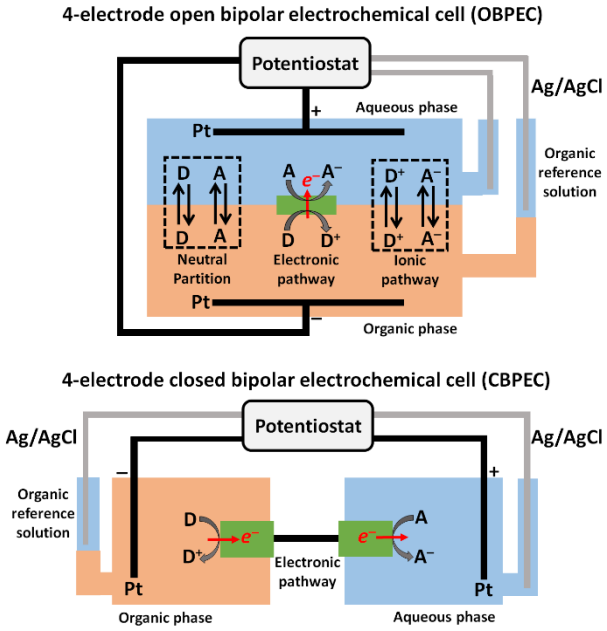

Scheme 1 Simplified schematics of the 4-electrode open bipolar electrochemical cell (OBPEC) and 4-electrode closed bipolar electrochemical cell (CBPEC) configurations with immiscible aqueous-organic electrolyte solutions. In both configurations, each phase contains a platinum wire driving electrode and a silver/silver chloride (Ag/AgCl) *pseudo*-reference electrode. The bipolar electrode (BPE) in each configuration is illustrated in green. In the CBPEC configuration, the BPE consists of electron conductors in each compartment (for example, platinum, gold, or glassy carbon electrodes) connected to each other by an electric wire. "A" and "D" are redox active electron acceptor and donor species, respectively, of differing solubility. In this instance, "A" is a highly hydrophilic species and "D" is a highly lipophilic species.

electron transfer (through Fermi level equilibration)[30] between a lipophilic redox species in the organic phase and a hydrophilic redox species in the aqueous phase, *e.g.,* a lipophilic donor (D) and a hydrophilic acceptor (A) redox species as in Scheme 1. Floating BPEs have been prepared from films of metallic NPs,[29,31,32] carbon nanomaterials (*e.g.,* graphene, carbon nanotubes or their nanocomposites),[33–35] and inorganic nanomaterials (*e.g.,* MoS_2).[36–38] The Fermi level of the floating BPE, and therefore the rate and direction of the interfacial electron transfer reaction, can be adjusted by varying $\Delta_o^w \phi$ at the ITIES. The latter is known as "redox electrocatalysis" and has been reviewed in depth recently.[39,40] Using this approach, the catalysis of interfacial electron transfer between a lipophilic electron donor redox couple, ferrocenium cation/ferrocene (Fc^+/Fc), and the hydrophilic electron acceptor redox couple, ferri-/ferrocyanide ($[Fe^{(III)}(CN)_6]^{3-}/Fe^{(II)}(CN)_6]^{4-}$), has been studied.[29] Additionally, the reduction of either dissolved O_2 to hydrogen peroxide and water[31,41] or aqueous protons to H_2 gas[42,43] has been achieved by interfacial electron transfer from various lipophilic ferrocene-derivatives. Redox electrocatalysis of O_2 reduction was also utilized to study platinum NP impacts upon a microscopic immiscible aqueous-organic interface.[44] During each impact event, the individual platinum NPs act as transient BPEs facilitating redox electrocatalysis and thereby extending the field of NP impact studies to encompass polarized immiscible aqueous-organic interfaces.[44]

By comparison, considerably fewer studies have been performed using immiscible aqueous-organic electrolyte solutions in a 4-electrode CBPEC configuration. The pioneering

work in this area was performed by Hotta *et al.* who studied electron transfer between lipophilic Fc^+/Fc in nitrobenzene and aqueous $[Fe^{(III)}(CN)_6]^{3-}/Fe^{(II)}(CN)_6]^{4-}$ by cyclic voltammetry.[27] The acronym "ECSOW" meaning "electron conductor separating oil-water" was chosen for these experiments. The BPE consisted of two platinum disk electrodes, one in each compartment, connected with an electric wire. In the 4-electrode CBPEC configuration with immiscible aqueous-organic solutions, the BPE is not connected to the potentiostat, so its internal potential is electrically ''floating''. Nonetheless, the electric currents flowing through the surfaces of the opposite poles of the BPE should be identical.[27] Other systems investigated include the electrodeposition of gold NPs by electron transfer from the lipophilic reductant triphenylamine to aqueous gold chloride precursor molecules,[45] and O_2 reduction in the aqueous compartment by electron transfer from lipophilic ferrocene-derivatives.[31,32] Furthermore, in related studies, Nishi and co-workers employed the 4-electrode CBPEC configuration to study electron transfer from decamethylferrocene dissolved in a superhydrophobic ionic liquid to aqueous gold or platinum chloride precursor molecules.[46,47]

Without exception, the motivation to perform experiments using immiscible aqueous-organic electrolyte solutions in a 4-electrode CBPEC configuration has been to provide mechanistic insight into the analogous interfacial electron transfer events taking place at the ITIES. In this regard, the CBPEC configuration significantly simplifies the biphasic experimental system by eliminating both the ionic pathway to conduct the electrochemical current and the partitioning of neutral species between the phases (see Scheme 1). However, as major fundamental differences between the systems exist, caution must be taken when extrapolating any insights from the CBPEC configuration to experimental findings at the ITIES. For example, while electron transfer between hydrophilic and lipophilic redox couples in a 4-electrode CBPEC configuration is thermodynamically equivalent to the corresponding interfacial electron transfer event at the ITIES, they may differ significantly from a kinetic viewpoint.[27] Thus, an electrochemically reversible redox reaction in the CBPEC configuration may be quasi-reversible or irreversible at the ITIES. Typically, the overpotential required to initiate electron transfer will be greater at the ITIES than in the CBPEC configuration. This is because a liquid-liquid junction with a mixed solvent region, *i.e.,* back-to-back diffuse double-layers, does not possess the same metallic behavior, with well-defined inner and outer double-layer regions, as is the case at the surface of each pole of the BPE in the CBPEC configuration. Thus, the onset potential for electron transfer between the two redox species on the Galvani potential scale recorded in the CBPEC configuration can only be used as a loose indicator of interfacial electron transfer occurring within the narrow ~1 V polarizable potential window available at the ITIES. Indeed, Hotta *et al.* recorded reversible CVs in the CBPEC configuration indicating electron transfer between Fc^+/Fc in nitrobenzene and aqueous $[Fe^{(III)}(CN)_6]^{3-}/Fe^{(II)}(CN)_6]^{4-}$ was thermodynamically feasible and possibly observable within the polarizable potential window at the ITIES.[27] However, with the aid of simulations, it has been shown that this thermodynamically expected interfacial electron transfer event does not take place at the ITIES.[48,49] Instead, electron transfer proceeds almost solely by the partitioning of neutral Fc followed by homogeneous electron transfer in the aqueous phase, and finally by the transfer of Fc^+ into the organic phase.[48,49] The latter ion transfer event at the ITIES generates a current within the polarizable potential window that may be easily confused with the current expected for interfacial electron transfer.

The interpretation of CVs for a 4-electrode CBPEC system is non-trivial as their features are determined by factors that influence the redox processes at both poles of the BPE simultaneously. As discussed in detail in Section 4, examples of factors that may introduce significant asymmetry in the redox processes occurring at each pole of the BPE are the redox potential of each redox couple, the rate constant of electron transfer at each pole, the presence of an excess bulk concentration of one redox couple over the other, and the relative areas of the poles of the BPE in contact with each electrolyte solution. In this regard, future studies involving finite element simulations of the full bipolar system will be essential to truly elucidate the observed, or expected, electrochemical response.

Closed bipolar electrochemistry in a 4-electrode configuration with immiscible aqueous-organic electrolyte solutions is an under-utilized technique with major potential to emerge as a powerful new methodology for electroanalysis. To date the use of BPEs for electroanalysis has primarily been concerned with all-aqueous based systems, both in the OBPEC and CBPEC configurations. The basic electroanalytical operating principle involves one pole of the BPE being the sensing device and the other pole being the reporting device.[50] At the opposite poles of the BPE, the currents for the oxidation and reduction half-reactions (discussed in detail *vide infra*) are equal and, thus, the signal generated at the reporting pole is an accurate reflection of the processes occurring at, and the state of, the sensing pole. A major distinguishing factor of using BPEs in electroanalysis is the decoupled nature of the sensing and reporting elements of the device. The reporting signal to date has primarily been the detection of an optical signal generated by the oxidation half-reaction, with the sensing being through the reduction half-reaction. Examples of the reporting signal include electrochemiluminescence (ECL),[51–53] electrochromism,[54–56] and electro-fluorescence.[57,58] Furthermore, the BPE can be miniaturized to the nanoscale, opening up opportunities for novel single molecule detection strategies.[59–61]

A major obstacle to the widespread adoption of closed bipolar electrochemistry in a 4-electrode configuration (especially with immiscible aqueous-organic electrolyte solutions) is the absence of a commercially available, easy-to-use electrochemical cell. In this regard, Colina and co-workers[62] fabricated a novel, highly versatile bipolar device consisting of a single conductor contacting droplets of two separate electrolyte solutions. This device was coupled with UV/vis and Raman spectroscopy and used to spectro-electrochemically monitor electron transfer between species in each electrolyte droplet, *e.g.,* between two aqueous redox couples, tris(2,2'-

bipyridine)ruthenium and potassium hexacyanoferrate, or redox couples in different solvents, such as 1,1'-dimethylferrocene in 1,2-dichlorobenzene and aqueous potassium hexacyanoferrate.

Further perspective uses of bipolar electrochemistry in a 4-electrode CBPEC configuration include the development of novel photo-electrochemical and *pseudo*-capacitive systems. Photo-induced interfacial electron transfer has been comprehensively investigated at the ITIES.[63] Electron transfer between certain redox species dissolved in the organic phase (*e.g.,* dimethylferrocene) and those in an aqueous phase (*e.g.,* dissolved oxygen) may proceed under illumination *via* a photoactive species at the ITIES. The latter were typically either a porphyrin,[64–67] semiconductor,[68–70] or dye-sensitized semiconductor.[71] Such experiments in a 4-electrode CBPEC configuration will be possible by sensitizing one of the poles of a BPE with such photoactive species, and dissolving appropriate redox species in each phase. An input of energy from light, in conjunction with polarizing the 4-electrode CBPEC system, must be required to facilitate electron transfer along the BPE. In other words, electron transfer between the redox species in the separate electrolyte solutions should be thermodynamically up-hill to ensure the conversion of light energy to chemical energy.[72]

Dryfe and co-workers demonstrated the interfacial doping of single-walled carbon nanotube (SWCNT) films at the ITIES in a 4-electrode OBPEC configuration to create a novel liquid-liquid *pseudo*-capacitor.[73] The concept involves interfacial electron transfer between a redox species dissolved in the organic phase (dimethylferrocene) and one in the aqueous phase ($[Fe^{(III)}(CN)_6]^{3-}/Fe^{(II)}(CN)_6]^{4-}$) *via* the SWCNT film. *In situ* Raman spectroscopy supported the hypothesis of electrochemical doping of the interfacial SWCNT film due to the charge transfer. Thus, novel *pseudo*-capacitors may be developed by immobilizing nanoscopic SWCNT films on one pole of the BPE, dissolving the appropriate redox species in each compartment, and polarizing the resulting 4-electrode CBPEC system to drive electron transfer along the BPE.

The ability to use a 4-electrode CBPEC with redox species dissolved in the same solvent in each compartment or in immiscible aqueous-organic solutions requires a thorough knowledge of the thermodynamics and kinetics of the half-reactions occurring at opposite poles of the BPE in each compartment. Thus, the primary aim in the remainder of this perspective is to provide a comprehensive overview of the influence of external bias on the thermodynamics underpinning electron transfer between redox species spatially separated in different compartments, along a conducting BPE.

3. Fermi levels of the electrons of the redox couples in solution and maintaining electroneutrality in each phase with a 4-electrode closed bipolar electrochemical cell

In this section we discuss the concept of the Fermi levels of the electrons of the redox couples in solution in each compartment and the mechanism of maintaining electroneutrality in each phase as electrons flow from one compartment to the other along the BPE under external polarization with a 4-electrode CBPEC configuration (see Scheme 2).

The Fermi level in solution (S) of a redox couple (Ox/Red), $E^{\mathrm{S}}_{\mathrm{F,Ox/Red}}$, is the work to bring an electron from vacuum (zero energy) onto the redox couple in solution (negative energy).[30,40] $E^{\mathrm{S}}_{\mathrm{F,Ox/Red}}$ is the electrochemical potential of an electron in Ox/Red in solution S, $\widetilde{\mu}^{\mathrm{S}}_{e^-}$, and, with the aid of a virtual redox reaction ($\mathrm{Ox_S} + e^{-,\mathrm{S}} \rightleftharpoons \mathrm{Red_S}$), can be defined as the difference between the electrochemical potentials of the oxidized and reduced species ($\widetilde{\mu}^{\mathrm{S}}_{e^-} = \widetilde{\mu}^{\mathrm{S}}_{\mathrm{Red}} - \widetilde{\mu}^{\mathrm{S}}_{\mathrm{Ox}}$). Meanwhile, from the Nernst equation, the standard redox potential of the redox reaction with an electron at rest in vacuum ($\mathrm{Ox_S} + e^{-,\mathrm{V}} \rightleftharpoons \mathrm{Red_S}$) is:

$$e\left[E^{\ominus}_{\mathrm{Ox/Red}}\right]^{\mathrm{S}}_{\mathrm{AVS}} = -\Delta G^{\ominus}_{\mathrm{Red}} = \mu^{\ominus,\mathrm{S}}_{\mathrm{Ox}} - \mu^{\ominus,\mathrm{S}}_{\mathrm{Red}} \quad (1)$$

where AVS is the absolute vacuum scale and the superscript $\ominus$ refers to the standard state. Therefore, $E^{\mathrm{S}}_{\mathrm{F,Ox/Red}}$ can be defined as:

$$E^{\mathrm{S}}_{\mathrm{F,Ox/Red}} = \widetilde{\mu}^{\mathrm{S}}_{e^-} = -e\left[E^{\ominus}_{\mathrm{Ox/Red}}\right]^{\mathrm{S}}_{\mathrm{AVS}} - e\phi^{\mathrm{S}} \quad (2)$$

where $\phi^{\mathrm{S}} = \chi^{\mathrm{S}} + \psi^{\mathrm{S}}$, with ϕ^{S} being the Galvani (inner) potential of the phase S composed of χ^{S}, the surface potential, and ψ^{S}, the outer potential, of solution S. $\widetilde{\mu}^{\mathrm{S}}_{e^-}$ may be expressed as follows:

$$\widetilde{\mu}^{\mathrm{S}}_{e^-} = \mu^{\mathrm{S}}_{e^-} - e\phi^{\mathrm{S}} = \mu^{\mathrm{S}}_{e^-} - e\left(\chi^{\mathrm{S}} + \psi^{\mathrm{S}}\right) = \alpha^{\mathrm{S}}_{e^-} - e\psi^{\mathrm{S}} \quad (3)$$

with $\alpha^{\mathrm{S}}_{e^-} = \mu^{\mathrm{S}}_{e^-} - e\chi^{\mathrm{S}}$. If solution S has no surface charge then $\psi^{\mathrm{S}} = 0$, and $\widetilde{\mu}^{\mathrm{S}}_{e^-}$ equates to the real chemical potential ($\alpha^{\mathrm{S}}_{e^-}$). Thus, the real chemical potential of an electron in a redox couple (Ox/Red) is the work to bring an electron into an *uncharged* solution S, *i.e.,* equivalent to the negative of the work function of solution S, $\alpha^{\mathrm{S}}_{e^-} = -\Phi^{\mathrm{S}}$. In the case of a system with multiple redox couples, all redox active species are in equilibrium, and typically one redox species in excess will dominate the Fermi level in solution S.

Let us consider a heterogeneous redox reaction between two redox couples, one in the aqueous compartment (w) and the other in organic compartment (o), *via* the BPE that electronically connects each solution. Overall, the heterogeneous redox reaction is:

$$n_{\mathrm{w}}\mathrm{D}^0_{\mathrm{o}} + n_{\mathrm{o}}\mathrm{A}^0_{\mathrm{w}} \rightleftharpoons n_{\mathrm{w}}\mathrm{D}^{n_{\mathrm{o}}+}_{\mathrm{o}} + n_{\mathrm{o}}\mathrm{A}^{n_{\mathrm{w}}-}_{\mathrm{w}} \quad (4)$$

where $\mathrm{A}^0_{\mathrm{w}}$ and $\mathrm{A}^{n_{\mathrm{w}}-}_{\mathrm{w}}$ are the oxidized and reduced forms of the aqueous electron acceptor, $\mathrm{D}^0_{\mathrm{o}}$ and $\mathrm{D}^{n_{\mathrm{o}}+}_{\mathrm{o}}$ are the oxidized and reduced forms of the organic electron donor, and n_{w} and n_{o} are the number of electrons exchanged for the aqueous and organic redox couples, respectively. The overall reaction is considered as oxidation and reduction half-reactions proceeding at opposite poles of the BPE in the organic ($\mathrm{BPE_o}$) and aqueous ($\mathrm{BPE_w}$) compartments, respectively:

$$n_{\mathrm{w}}\mathrm{D}^0_{\mathrm{o}} + \mathrm{BPE}^z_{\mathrm{o}} \rightleftharpoons n_{\mathrm{w}}\mathrm{D}^{n_{\mathrm{o}}+}_{\mathrm{o}} + \mathrm{BPE}^{z-(n_{\mathrm{w}}\cdot n_{\mathrm{o}})}_{\mathrm{o}} \quad (5)$$

$$n_{\mathrm{o}}\mathrm{A}^0_{\mathrm{w}} + \mathrm{BPE}^{z-(n_{\mathrm{w}}\cdot n_{\mathrm{o}})}_{\mathrm{w}} \rightleftharpoons n_{\mathrm{o}}\mathrm{A}^{n_{\mathrm{w}}-}_{\mathrm{w}} + \mathrm{BPE}^z_{\mathrm{w}} \quad (6)$$

where z is the charge on the poles of the BPEs. At equilibrium, the Fermi level of the electrons in the aqueous redox couple ($E^{\mathrm{w}}_{\mathrm{F,}\,\mathrm{A}^0_{\mathrm{w}}/\mathrm{A}^{n_{\mathrm{w}}-}_{\mathrm{w}}}$) is equal to that in the organic redox couple ($E^{\mathrm{o}}_{\mathrm{F,}\,\mathrm{D}^{n_{\mathrm{o}}+}_{\mathrm{o}}/\mathrm{D}^0_{\mathrm{o}}}$). $E^{\mathrm{w}}_{\mathrm{F,}\,\mathrm{A}^0_{\mathrm{w}}/\mathrm{A}^{n_{\mathrm{w}}-}_{\mathrm{w}}}$ is given by the Nernst equation and the Galvani potential of water (known as the inner potential, ϕ^{w}) on the AVS taking the electron at rest in the vacuum as the origin (in kJ·mol^{-1}; note that Eqns (1) to (3) are in terms of one

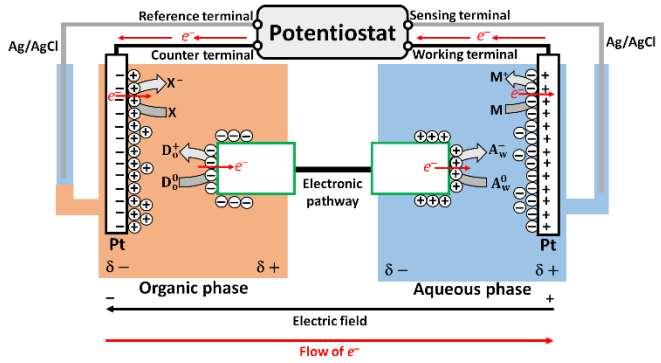

Scheme 2 Detailed schematic of the 4-electrode closed bipolar electrochemical cell (CBPEC) configuration with immiscible aqueous-organic electrolyte solutions as the Galvani potential difference between the aqueous and organic phases ($\Delta_o^w\phi$) is biased positively by the potentiostat. The schematic highlights the terminals of the potentiostat connected to each driving or reference electrode, the build-up of electrochemical double-layers at each electrode surface and the redox reactions at each pole of the bipolar electrode immersed in the aqueous and organic electrolyte solutions, and the redox reactions taking place at the surface of each driving electrode to maintain electroneutrality in each phase at all times.

species, while from Eqn (7) onwards the equations are expressed with respect to one mole of species with $F = eN_a$):

$$E^{w}_{F,\,A^0_w/A^{n_w-}_w} = -F\left[\left[E^{\ominus}_{A^0_w/A^{n_w-}_w}\right]^{w}_{SHE} + \frac{RT}{n_wF}\ln\left(\frac{c^b_{A^0_w}}{c^b_{A^{n_w-}_w}}\right) + \phi^{w} + \left[E^{\ominus}_{H^+/{}^1/_2H_2}\right]^{w}_{AVS}\right] \quad (7)$$

where $\left[E^{\ominus}_{H^+/{}^1/_2H_2}\right]^{w}_{AVS} = 4.44$ V is the potential of the standard hydrogen electrode (SHE) on the AVS, $\left[E^{\ominus}_{A^0_w/A^{n_w-}_w}\right]^{w}_{SHE}$ is the standard redox potential of the aqueous electron acceptor, n_w is the number of electrons exchanged in Eqn (6), $c^b_{A^0_w}$ and $c^b_{A^{n_w-}_w}$ are the bulk concentrations of the oxidized and reduced forms, respectively, of the electron acceptor in the aqueous solution and, finally, ϕ^w the Galvani (inner) potential is defined by $\phi^w = \chi^w + \psi^w$, where χ^w is the surface potential and ψ^w is the outer potential of the aqueous phase. It is not possible to measure the Galvani potential of a phase, so the absolute value of $E^{w}_{F,\,A^0_w/A^{n_w-}_w}$ is not known. However, using a 4-electrode electrochemical cell, it is possible to control the Galvani potential difference ($\Delta_o^w\phi$) between the aqueous and organic compartments. Similarly, $E^{o}_{F,\,D^{n_o+}_o/D^0_o}$ is given by:

$$E^{o}_{F,\,D^{n_o+}_o/D^0_o} = -F\left[\left[E^{\ominus}_{D^{n_o+}_o/D^0_o}\right]^{o}_{SHE} + \frac{RT}{n_oF}\ln\left(\frac{c^b_{D^{n_o+}_o}}{c^b_{D^0_o}}\right) + \phi^{o} + \left[E^{\ominus}_{H^+/{}^1/_2H_2}\right]^{w}_{AVS}\right] \quad (8)$$

Electron flow along the BPE only takes place from a higher Fermi level into a lower Fermi level, *i.e.,* for electrons to flow, $E^{o}_{F,\,D^{n_o+}_o/D^0_o} > E^{w}_{F,\,A^0_w/A^{n_w-}_w}$. However, even when the latter thermodynamic requirement is satisfied, without external bias of the driving electrodes in each phase no current flows from one pole of the BPE to the other. *Current may only flow along the BPE in a CBPEC configuration if a mechanism is in place to compensate the loss of charge from one compartment and the commensurate gain of charge in the other compartment.* In other words, for electrons to flow along the BPE, *electroneutrality* must be maintained in each compartment at all times (see Scheme 2).

Typically, in electrochemical systems such as Galvanic cells, electroneutrality is maintained by introducing a salt bridge. Thus, the equilibrium potential difference between the redox couples in both compartments drives an electronic current between the electrodes in each phase, with an ionic current of identical magnitude but opposite direction flowing across the salt bridge. Conceptually, the two compartments in the 4-electrode CBPEC system may be considered as two back-to-back 3-electrode electrochemical cells connected by an electronic bridge, *i.e.,* the BPE. The pole of the BPE in each electrolyte solution acts as a working electrode, with the driving electrode in each electrolyte solution acting as a counter electrode. In a 3-electrode cell, for current to flow at the working electrode, external polarization is required to drive the opposite redox process at the counter electrode. In this way, the electroneutrality of the electrolyte solution is maintained while current flows simultaneously at both the working and counter electrodes. Analogously, in the 4-electrode CBPEC, external polarization of the driving electrodes is required to maintain electroneutrality. Thus, when electrons flow along the BPE, electroneutrality is maintained in each compartment throughout by redox reactions occurring at the surface of each driving electrode (see Scheme 2). Consequently, if a reduction reaction occurs at the negative pole of the BPE, an oxidation reaction will occur at the driving electrode in that compartment.

For the 4-electrode CBPEC with immiscible aqueous-organic solutions, the organic driving and reference electrodes are connected to the counter and reference terminals of the potentiostat, respectively, while the aqueous driving and reference electrodes are connected to the working and sensing terminals, respectively (see Scheme 2). The potentiostat monitors $\Delta_o^w\phi$ between the reference electrodes at the sensing (which senses ϕ^w) and reference (which senses ϕ^o) terminals. $\Delta_o^w\phi$ is controlled externally by independently "driving" current through the driving electrodes at the counter and working terminals (and thus changing their potentials) to vary ϕ^o relative to ϕ^w, respectively.

Positive external polarization of $\Delta_o^w\phi$ means ϕ^w shifts positively with respect to ϕ^o, or ϕ^o shifts negatively with respect to ϕ^w. This may be achieved by applying the needed external voltage between the driving electrodes, such that the required potential difference between the sensing and reference electrodes, *i.e.,* $\Delta_o^w\phi$, is satisfied. Consequently, in the aqueous phase, the positive charge at the surface of the driving electrode is compensated by the build-up of an electrochemical double-layer rich in anions. Meanwhile, in the organic phase, the opposite trend occurs, with an electrochemical double-layer rich in cations building up at the surface of the driving electrode. The polarized driving electrodes induce redox reactions at their surfaces. Thus, a molecule M (solvent, electrolyte or redox active molecule), will be oxidized to M^+ at the surface of the aqueous driving electrode, and a molecule X (solvent, electrolyte or redox active molecule) will be reduced to X^- at the surface of the organic driving electrode (Scheme 2). These redox reactions take place far from the surface of each pole of the BPE and any products formed do not influence the electrochemical reactions taking place at the surface of the BPE. As depicted in Scheme 2, if we consider each compartment in isolation, the

aqueous pole of the BPE experiences a relatively negative electric field (δ–) at its location within that compartment, whereas the organic pole of the BPE experiences a relatively positive electric field (δ+). Thus, cations migrate towards the aqueous pole of the BPE, forming a cation rich layer at its surface, and anions migrate towards the organic pole of the BPE (Scheme 2).

Let's now consider the situation when $\Delta_{\mathrm{o}}^{\mathrm{w}}\phi$ is polarized sufficiently positive to induce electron transfer between two redox couples, one in each compartment, as described in Eqns (4) to (6). In the organic compartment, $\mathrm{D_o^0}$ will be oxidized at the organic pole of the BPE, see Eqn (5), with the concurrent reduction of molecule X at the surface of the driving electrode maintaining electroneutrality (Scheme 2). Simultaneously, in the aqueous compartment, $\mathrm{A_w^0}$ will be reduced at the aqueous pole of the BPE, see Eqn (6), with the concurrent oxidation of molecule M at the surface of the driving electrode maintaining electroneutrality (Scheme 2).

4. Experimental variables that influence the position of the Line of Zero Overpotential (LZO) on the BPE at steady-state conditions under an external bias

In this section, we discuss the equilibrium Galvani potential difference established between the aqueous and organic poles of the BPE both prior to and after application of an external bias. Furthermore, we introduce the concept of the Line of Zero Overpotential (LZO) and the thermodynamic theory outlining how various experimental variables can influence the position of the LZO on the BPE at steady-state conditions under an external bias. This theory builds on previous work regarding "redox electrocatalysis" by conductive floating BPEs, *i.e.,* a film of gold NPs at the liquid-liquid interface, in a 4-electrode OBPEC with immiscible aqueous-organic solutions.[29,31]

An electric field is established between the two driving electrodes upon external polarization. The magnitude of the electric field varies at each location along the BPE in parallel to the driving electric field. However, a key point is that *the BPE is an equipotential body* and has a floating potential or Fermi level ($E_{\mathrm{F,BPE}}$). The aqueous and organic electrolyte solutions are polarized in the presence of an applied electric field and *the magnitude of the potential drop across the organic phase far exceeds that taking place in the aqueous phase*. This is because the aqueous and organic phases are fundamentally different in terms of their conductivities, with a much larger *i*R drop experienced in the organic phase. The typical organic phases utilized in OBPEC experiments, 1,2-dichloroethane and α,α,α-trifluorotoluene, have much lower relative permittivities (ε = 10.4 and 9.2, respectively)[39] than water (ε = 80.1) at 20°C. Additionally, the usual organic electrolyte salt employed, bis(triphenylphosphoranylidene) ammonium tetrakis(pentafluorophenyl)borate, is poorly dissociated into its constituent ions in organic solvents by comparison with an aqueous electrolyte salt, such as sodium chloride (NaCl), which completely dissociates in water.

When the BPE is brought in contact with the aqueous and organic solutions, prior to polarization using a potentiostat (designated herein as time zero, t = 0), a potential difference between the aqueous and organic solutions, *i.e.,* an equilibrium Galvani potential difference ($\Delta_{\mathrm{o}}^{\mathrm{w}}\phi_{\mathrm{eq.}}^{t=0}$), is immediately established and defined as:

$$[\phi^{w}-\phi^{o}]_{\mathrm{eq}} = \Delta_{\mathrm{o}}^{\mathrm{w}}\phi_{\mathrm{eq.}}^{t=0}$$
$$\Delta_{\mathrm{o}}^{\mathrm{w}}\phi_{\mathrm{eq.}}^{t=0} = \left[E_{\mathrm{D_o^{n_o+}/D_o^0}}\right]_{\mathrm{SHE}}^{\mathrm{o}} - \left[E_{\mathrm{A_w^0/A_w^{n_w-}}}\right]_{\mathrm{SHE}}^{\mathrm{w}}$$
$$\Delta_{\mathrm{o}}^{\mathrm{w}}\phi_{\mathrm{eq.}}^{t=0} = \Delta_{\mathrm{o}}^{\mathrm{w}}\phi_{\mathrm{HET}}^{\ominus} + \frac{RT}{(n_{\mathrm{w}}\cdot n_{\mathrm{o}})F}\ln\left(\frac{c_{\mathrm{A_w^{n_w-}}}^{b}}{c_{\mathrm{A_w^0}}^{b}}\right)^{n_{\mathrm{o}}}\left(\frac{c_{\mathrm{D_o^{n_o+}}}^{b}}{c_{\mathrm{D_o^0}}^{b}}\right)^{n_{\mathrm{w}}} \quad (9)$$

where $\Delta_{\mathrm{o}}^{\mathrm{w}}\phi_{\mathrm{HET}}^{\ominus}$ is the standard Galvani potential difference for the heterogeneous electron transfer (HET), given by:

$$\Delta_{\mathrm{o}}^{\mathrm{w}}\phi_{\mathrm{HET}}^{\ominus} = \left[E_{\mathrm{D_o^{n_o+}/D_o^0}}^{\ominus}\right]_{\mathrm{SHE}}^{\mathrm{o}} - \left[E_{\mathrm{A_w^0/A_w^{n_w-}}}^{\ominus}\right]_{\mathrm{SHE}}^{\mathrm{w}} \quad (10)$$

Thus, at t = 0, the BPE is in contact with both phases, and due to the absence of current, an equilibrium Galvani potential difference ($\Delta_{\mathrm{o}}^{\mathrm{w}}\phi_{\mathrm{eq.}}^{t=0}$) between the two phases is established. However, in the absence of an applied external bias between the drivin electrodes at t = 0, electrons cannot flow to establish a new equilibrium due to the lack of a mechanism to maintain electroneutrality in each phase, as discussed *vide supra*. Only by polarizing the driving electrodes in the 4-electrode CBPEC with immiscible aqueous-organic solutions using an external power supply, can we change the potential of the aqueous redox couple *with respect to* the organic redox couple at the surface of the BPE, or $E_{\mathrm{F,\,A_w^0/A_w^{n_w-}}}^{\mathrm{w}}$ with respect to $E_{\mathrm{F,\,D_o^{n_o+}/D_o^0}}^{\mathrm{o}}$. In other words, by external polarization, we are varying the $e\phi^{S}$ term in Eqn (2) for a single species, thus changing $\Delta_{\mathrm{o}}^{\mathrm{w}}\phi$. For one mole of species, we are shifting ϕ^{o} negatively with respect to ϕ^{w}, and therefore $E_{\mathrm{F,\,D_o^{n_o+}/D_o^0}}^{\mathrm{o}}$ positively with respect to $E_{\mathrm{F,\,A_w^0/A_w^{n_w-}}}^{\mathrm{w}}$, see Eqns (7) and (8). Thus, a new value of $\Delta_{\mathrm{o}}^{\mathrm{w}}\phi_{\mathrm{eq.}}^{t=x}$ is established at time x (t = x), with a greater potential difference between $E_{\mathrm{F,\,D_o^{n_o+}/D_o^0}}^{\mathrm{o},t=x}$ and $E_{\mathrm{F,\,A_w^0/A_w^{n_w-}}}^{\mathrm{w},t=x}$ than was the case at t = 0. Under external polarization, to establish a new equilibria between $E_{\mathrm{F,\,A_w^0/A_w^{n_w-}}}^{\mathrm{w}}$ and $E_{\mathrm{F,\,D_o^{n_o+}/D_o^0}}^{\mathrm{o}}$, the surface concentration ratios of the organic donor ($c_{\mathrm{D_o^{n_o+}}}^{S}/c_{\mathrm{D_o^0}}^{S}$) and aqueous acceptor ($c_{\mathrm{A_w^0}}^{S}/c_{\mathrm{A_w^{n_w-}}}^{S}$) redox species adjust at the organic and aqueous poles of the BPE, respectively, by electrons flowing along the BPE. From the Nernst equation, the latter changes the potential of the aqueous redox couple *with respect to* the organic redox couple.

The driving force or overpotential (in volts) for the cathodic reduction reaction at each location on the aqueous pole of the BPE is the difference between the Fermi levels of the electrons in the BPE and the electrons in the aqueous redox acceptor species:

$$\eta_{\mathrm{cat.}} = \frac{\left(E_{\mathrm{F,BPE}} - E_{\mathrm{F,\,A_w^0/A_w^{n_w-}}}^{\mathrm{w}}\right)}{F} \quad (11)$$

Similarly, the overpotential for the anodic oxidation reaction at each location on the organic pole of the BPE:

$$\eta_{\mathrm{an.}} = \frac{-\left(E_{\mathrm{F,BPE}} - E_{\mathrm{F,\,D_o^{n_o+}/D_o^0}}^{\mathrm{o}}\right)}{F} \quad (12)$$

It is important to note, that as in any double-layer between a solid and an electrolyte solution, the potential difference or overpotential in this case, has a distribution normal to the electrode surface. Therefore, only redox couples close to the surface of each pole of the BPE experience this force. Thus, the equilibrium Galvani potential difference between any two locations on the anodic organic and cathodic aqueous poles of the BPE in parallel to the electric field is equal to the sum of the overpotentials for the anodic and cathodic reactions at those

locations. Prior to the external application of an electric field at t = 0, $\Delta_o^w\phi_{eq.}^{t=0} = \eta_{an.}^{t=0} + \eta_{cat.}^{t=0}$ between all locations on the aqueous and organic poles of the BPE. Subsequently, upon varying $\Delta_o^w\phi$ to a new fixed value at $t = x$, $\Delta_o^w\phi_{eq.}^{t=x} = \eta_{an.}^{t=x} + \eta_{cat.}^{t=x}$ is maximized at the extremities of the aqueous and organic poles of the BPE.

The rates of both the oxidation and reduction electrochemical half-reactions under external bias can be considered to follow Butler-Volmer kinetics using the Fermi levels of solid electrodes and redox couples in solution instead of electrode potentials. These rates are governed by an exponential term dependent on the driving force (*i.e.,* either $\eta_{cat.}$ or $\eta_{an.}$), the rate constant, k^0 (which is independent of the overpotential), and the surface concentrations of the reactant species.

Comparisons of the effects of external bias on the Fermi levels of the electrons in solution, and subsequently the thermodynamics of Fermi level equilibration between electron donor and acceptor redox couples at opposite poles of the BPE, are shown for 4-electrode CBPECs with aqueous electrolyte solutions in both compartments (Scheme 3A) or with immiscible aqueous-organic electrolyte solutions (Schemes 3B and C). At t = x under the same external bias and between identical locations on the BPE, a higher equilibrium Galvani potential difference is induced when the redox couples are dissolved separately in non-identical aqueous-organic solvents ($\Delta_o^w\phi_{eq.}^{t=x}$), rather than in identical aqueous solutions ($\Delta\phi_{eq.}^{t=x}$). The latter is due to the magnitude of the potential drop across the organic phase far exceeding that across the aqueous phase, as discussed *vide supra*, and therefore in turn the magnitude of $\eta_{an.}^{t=x}$ being greater for an electron donor dissolved in an organic electrolyte solution than in an aqueous electrolyte solution, see Scheme 3A(i) and B(i). Thus, a major advantage of using non-identical solvents is the lower electric field necessary to establish a significant equilibrium Galvani potential difference between the extremities of the BPE in order to drive the bipolar redox reaction with satisfactory kinetics.

The following discussion focusses on the use of a 4-electrode CBPEC with immiscible aqueous-organic solutions and the electron donor species dissolved in the organic compartment, as depicted in Scheme 3B. However, all aspects of this discussion are equally applicable to a 4-electrode CBPEC with aqueous solutions in both compartments, as depicted in Scheme 3A, by simply substituting the relevant terms. As the reactions at the opposite ends of the BPE in each compartment proceed, from t = x, when $\Delta_o^w\phi$ was initially varied by external polarization, until a steady-state or equilibrium between the anodic and cathodic half-reactions is reached, defined as time equal to infinity (t = ∞), the position of $E_{F,BPE}$ constantly shifts. During this time, electrons flow from the organic to aqueous compartments as described in Eqns (5) and (6), with $E^o_{F,\,D_o^{no+}/D_o^0}$ lowering (Scheme 3B(ii), orange arrow) and $E^w_{F,\,A_w^0/A_w^{nw-}}$ rising (Scheme 3B(ii), blue arrow) as the organic donor $c^s_{D_o^{no+}}/c^s_{D_o^0}$ and aqueous acceptor $c^s_{A_w^0}/c^s_{A_w^{nw-}}$ surface concentration ratios adjust. Finally, at steady-state and under an applied bias, the Fermi level of the electrons in the BPE and the Fermi levels of the electrons in both solutions are equal. This equilibria may be defined as the LZO, with no net current flowing between either pole of the BPE [3], see Scheme 3B(ii), dashed line:

$$\text{LZO} = E_{F,BPE}^{t=\infty} = E^{w,t=\infty}_{F,\,A_w^0/A_w^{nw-}} = E^{o,t=\infty}_{F,\,D_o^{no+}/D_o^0} \quad (13)$$

If we assume that concentration polarization does not occur, no kinetic limitations to Fermi level equilibration are present, the back-reactions are negligible, and the BPE is chemically inert in both the aqueous and organic compartments, the current for both reactions at the opposite poles of the BPE should be identical. The current for the reduction half-reaction at the pole of the BPE in the aqueous compartment (i^w_{BPE}, see Eqn (6)) is:

$$i^w_{BPE} = -n_w A^w_{BPE} F k^0_w c^s_{A_w^0} e^{(1-\alpha_w)n_w\eta_{cat.}/RT} \quad (14)$$

where A^w_{BPE} is the area of the pole of the BPE in the aqueous compartment undergoing the electrochemical reaction described in Eqn (6), k^0_w is the potential-independent rate constant at the aqueous pole of the BPE, and α_w is the charge transfer coefficient in the aqueous phase (commonly close to 0.5).

Correspondingly, the current for the oxidation half-reaction at the pole of the BPE in the organic compartment (i^o_{BPE}, see Eqn (5)) is:

$$i^o_{BPE} = n_o A^o_{BPE} F k^0_o c^s_{D_o^0} e^{-\alpha_o n_o \eta_{an.}/RT} \quad (15)$$

Note that the oxidative current is defined as positive, in accordance with IUPAC definition. Also, the terms $\eta_{cat.}$ and $\eta_{an.}$ contain the Galvani potentials for both phases.

Thus, at steady-state conditions under an external bias, the LZO or $E^{t=\infty}_{F,BPE}$ can be defined as:

$$\text{LZO} = E^{t=\infty}_{F,BPE} = \frac{\left((1-\alpha_w)n_w E^w_{F,\,A_w^0/A_w^{nw-}} + \alpha_o n_o E^o_{F,\,D_o^{no+}/D_o^0}\right)}{\left((1-\alpha_w)n_w + \alpha_o n_o\right)} - \frac{RT}{\left((1-\alpha_w)n_w + \alpha_o n_o\right)} \ln\left[\frac{n_w A^w_{BPE} k^0_w c^s_{A_w^0}}{n_o A^o_{BPE} k^0_o c^s_{D_o^0}}\right] \quad (16)$$

Numerical methods are required if the back-reactions cannot be neglected as the situation becomes too complicated to be easily solved analytically. For simplicity, if $\alpha_w = \alpha_o = 0.5$ and $n_w = n_o = n$, then Eqn (16) simplifies to:

$$\text{LZO} = E^{t=\infty}_{F,BPE} = \frac{\left(E^w_{F,\,A_w^0/A_w^{nw-}} + E^o_{F,\,D_o^{no+}/D_o^0}\right)}{2} - \frac{RT}{n} \ln\left[\frac{A^w_{BPE} k^0_w c^s_{A_w^0}}{A^o_{BPE} k^0_o c^s_{D_o^0}}\right] \quad (17)$$

In Scheme 3B we discuss the scenario for a strong reductant in the organic phase, with $E^{o,t=0}_{F,\,D_o^{no+}/D_o^0} > E^{w,t=0}_{F,\,A_w^0/A_w^{nw-}}$, see Scheme 3B(i) and (ii), solid lines. In this situation, once electroneutrality is maintained in both phases by redox reactions at each driving electrode upon moderately biasing $\Delta_o^w\phi$ positively by external polarization, a significant $\Delta_o^w\phi_{eq.}^{t=x}$ is established and electrons should flow "spontaneously" along the BPE at t = x with fast kinetics, see Scheme 3B(i) and (ii), dotted lines. Let's now consider the scenario for a weak reductant in the organic phase, with $E^{o,t=0}_{F,\,D_o^{no+}/D_o^0} < E^{w,t=0}_{F,\,A_w^0/A_w^{nw-}}$, see Schemes 3C(i) and (ii), solid lines. In this situation, to force electron transfer to happen (both with a thermodynamic driving force and in practice with fast kinetics), a very large bias of $\Delta_o^w\phi$ using an external power source is applied such that the order of the Fermi levels of the redox species flips to $E^{o,t=x}_{F,\,D_o^{no+}/D_o^0} > E^{w,t=x}_{F,\,A_w^0/A_w^{nw-}}$, see Schemes 3C(i) and (ii), dotted lines. Now electron transfer proceeds until equilibrium is reached at t = ∞ and the LZO is defined, see Scheme 3C(ii), dashed line.

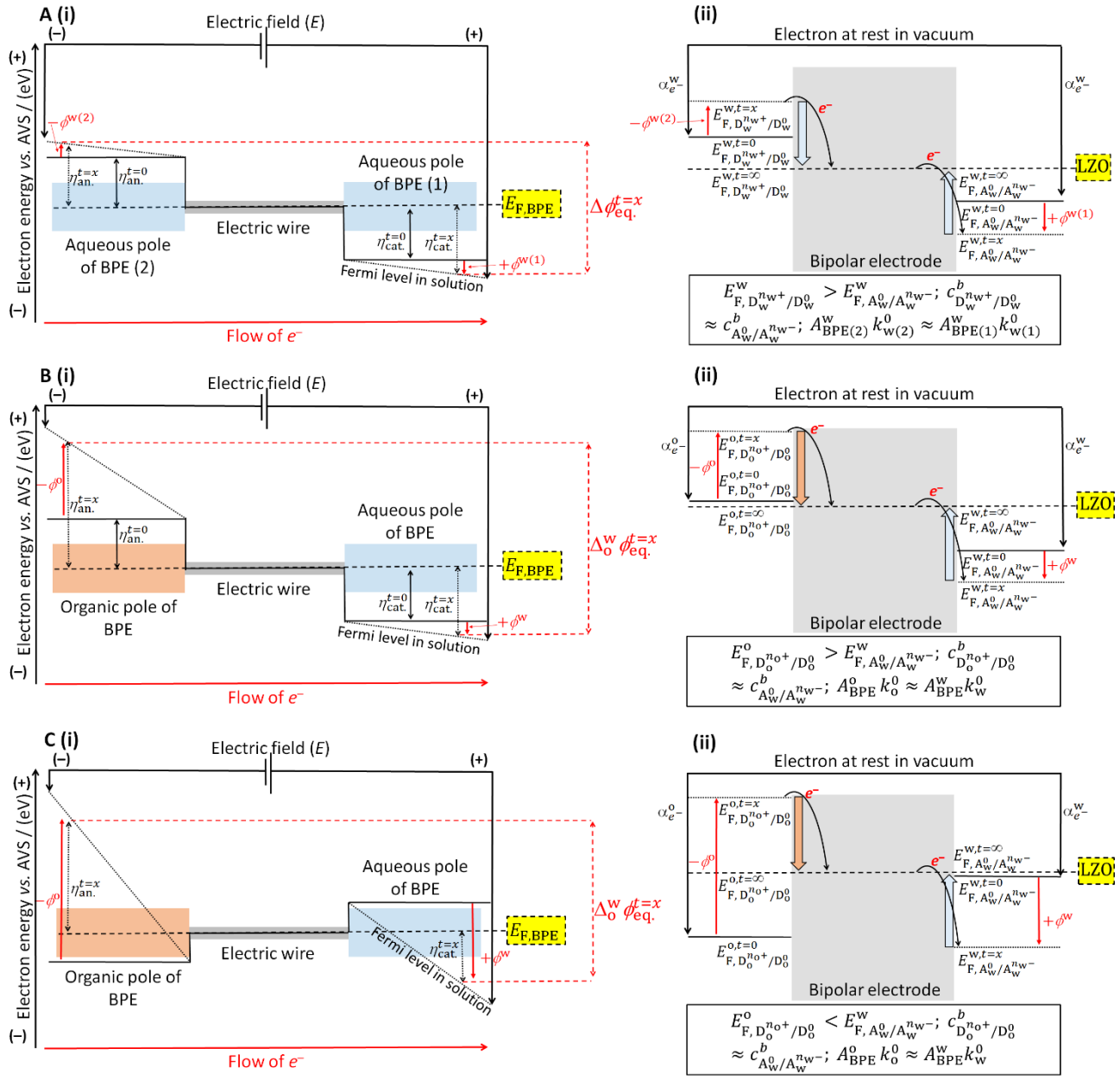

Scheme 3 Schematics comparing the effects of external bias on the Fermi levels of the electrons in solution (in each part (i)), and subsequently the thermodynamics of Fermi level equilibration between electron donor and acceptor redox couples at opposite poles of the BPE (in each part (ii)), are shown for 4-electrode CBPECs with aqueous electrolyte solutions in both compartments (**a**) or with immiscible aqueous-organic electrolyte solutions (**b, c**). For the 4-electrode CBPEC with aqueous electrolyte solutions in both compartments, the inner potentials of the two aqueous phases are designed as $\phi^{w(1)}$ and $\phi^{w(2)}$, respectively, and the equilibrium Galvani potential difference established on application of an external bias at $t = x$ is designated as $\Delta\phi_{eq.}^{t=x}$. The latter is designed as $\Delta_o^w\phi_{eq.}^{t=x}$ for the 4-electrode CBPECs with immiscible aqueous-organic solutions. In all schemes, the Fermi levels of the electrons in solution prior to the application of an external bias at $t = 0$ are represented by solid black lines, whereas on application of an external bias at $t = x$ they are represented as dotted black lines. The equilibrium positions at $t = \infty$ are represented by dashed black lines. The schematics of the 4-electrode CBPECs in (**a**) and (**b**) represent the scenario when the Fermi level of the electrons in the electron donor species is greater than the electron acceptor species, *i.e.*, for (**b**) $E_{F,D_o^{n_o+}/D_o^0}^{o,t=0} > E_{F,A_w^0/A_w^{n_w-}}^{w,t=0}$. The opposite scenario is depicted in (**c**) with $E_{F,D_o^{n_o+}/D_o^0}^{o,t=0} < E_{F,A_w^0/A_w^{n_w-}}^{w,t=0}$. In each part (ii), when the Galvani potential difference is biased sufficiently positive at time x using an external power source, the oxidation and reduction electrochemical half-reactions proceed at opposite ends of the BPE in each compartment from $t = x$ until equilibrium is reached at $t = \infty$ (note that in (**a**) $\Delta\phi = (\phi^{w(1)} - \phi^{w(2)})$ and in (**b, c**) $\Delta_o^w\phi = (\phi^w - \phi^o)$). During this time, the positions of the Fermi levels of the electrons in both solutions at the surface of the BPE lower (for the anodic half-reaction) or raise (for the cathodic half-reaction), as indicated by the orange and blue arrows. At equilibrium, under an applied external bias, the Fermi level of the electrons in the BPE and the Fermi levels of the electrons in both solutions at the surface of the BPE are equal. This is defined as the Line of Zero Overpotential (LZO) on the BPE. For schemes (**b**) and (**c**), as $c_{D_o^{n_o+}/D_o^0}^b \approx c_{A_w^0}^b/c_{A_w^{n_w-}}^b$ and $A_{BPE}^o k_o^0 \approx A_{BPE}^w k_w^0$, at equilibrium under an external bias, the LZO is found mid-way between $E_{F,A_w^0/A_w^{n_w-}}^{w,t=x}$ and $E_{F,D_o^{n_o+}/D_o^0}^{o,t=x}$. The same is true for scheme (**a**) with $c_{D_w^{n_w+}/D_w^0}^b \approx c_{A_w^0}^b/c_{A_w^{n_w-}}^b$ and $A_{BPE(2)}^w k_{w(2)}^0 \approx A_{BPE(1)}^w k_{w(1)}^0$.

If the bulk concentrations of the redox species, $c^b_{\mathrm{D_o}^{n_o+}}/c^b_{\mathrm{D_o^0}}$ and $c^b_{\mathrm{A_w^0}}/c^b_{\mathrm{A_w}^{n_w-}}$, are similar and concentration polarization is ignored, then the different relationships between $A^{\mathrm{w}}_{\mathrm{BPE}}k^0_{\mathrm{w}}$ and $A^{\mathrm{o}}_{\mathrm{BPE}}k^0_{\mathrm{o}}$ significantly influence the position of the LZO, as illustrated in Schemes 3 and 4, and discussed in detail *vide infra*. It is important to note, however, that the LZO will always be found between $E^{\mathrm{w}}_{\mathrm{F,\,A_w^0/A_w}^{n_w-}}$ and $E^{\mathrm{o}}_{\mathrm{F,\,D_o}^{n_o+}/\mathrm{D_o^0}}$. Firstly, if the areas for both reactions are the same at the opposite poles of the BPE ($A^{\mathrm{o}}_{\mathrm{BPE}} \approx A^{\mathrm{w}}_{\mathrm{BPE}}$) and both reactions proceed with similar potential-independent rate constants ($k^0_{\mathrm{o}} \approx k^0_{\mathrm{w}}$), then $A^{\mathrm{o}}_{\mathrm{BPE}}k^0_{\mathrm{o}} \approx A^{\mathrm{w}}_{\mathrm{BPE}}k^0_{\mathrm{w}}$ and under an applied bias the position of the LZO is half of the sum of the Fermi levels of the two redox couples at $t = x$. In other words, the LZO is exactly between $E^{\mathrm{o},t=x}_{\mathrm{F,\,D_o}^{n_o+}/\mathrm{D_o^0}}$ and $E^{\mathrm{w},t=x}_{\mathrm{F,\,A_w^0/A_w}^{n_w-}}$. This is the situation illustrated in Schemes 3B(ii) and C(ii). Slow kinetics for one of the reactions, for example the oxidation reaction, can be compensated if the area of the pole of the BPE in that compartment is very large. In this instance, $A^{\mathrm{o}}_{\mathrm{BPE}}k^0_{\mathrm{o}} \gg A^{\mathrm{w}}_{\mathrm{BPE}}k^0_{\mathrm{w}}$ but $k^0_{\mathrm{o}} \ll k^0_{\mathrm{w}}$, with the two opposite trends cancelling each other out and leading to a situation where $A^{\mathrm{o}}_{\mathrm{BPE}}k^0_{\mathrm{o}} \approx A^{\mathrm{w}}_{\mathrm{BPE}}k^0_{\mathrm{w}}$. Also, although $\Delta^{\mathrm{w}}_{\mathrm{o}}\phi_{\mathrm{eq.}}$ may increase, *e.g.,* at $t = x$ in Scheme 3B(ii), or invert, *e.g.,* at $t = x$ in Scheme 3C(ii), the position of the LZO remains in the middle.

It is worth noting that for a 4-electrode CBPEC with identical aqueous solutions in both compartments, when the LZO is exactly between $E^{\mathrm{w},t=x}_{\mathrm{F,\,D_w}^{n_w+}/\mathrm{D_o^0}}$ and $E^{\mathrm{w},t=x}_{\mathrm{F,\,A_w^0/A_w}^{n_w-}}$, applying a positive bias will affect the overpotentials for the oxidation and reduction half-reactions equally at each pole of the BPE, see Scheme 3A(i). Thus, for locations on the anodic organic and cathodic aqueous poles, equidistant from the mid-point of the BPE in parallel to the driving electric field, $\eta^{t=x}_{\mathrm{an.}} = \eta^{t=x}_{\mathrm{cat.}}$. This is not the case for a 4-electrode CBPEC with immiscible aqueous-organic solutions, once more due to the magnitude of the potential drop across the organic phase far exceeding that across the aqueous phase, as discussed *vide supra*, leading to $\eta^{t=x}_{\mathrm{an.}} > \eta^{t=x}_{\mathrm{cat.}}$ as shown in Scheme 3B(i).

Secondly, if $A^{\mathrm{o}}_{\mathrm{BPE}}k^0_{\mathrm{o}} \gg A^{\mathrm{w}}_{\mathrm{BPE}}k^0_{\mathrm{w}}$, additional driving force (overpotential) is required to drive the reduction half-reaction at the aqueous pole (Eqn (6)) at the same rate as the oxidation half-reaction at the organic pole (Eqn (5)). At steady-state under an external bias, the LZO is positioned close to $E^{\mathrm{o},t=x}_{\mathrm{F,\,D_o}^{n_o+}/\mathrm{D_o^0}}$, see Scheme 4A, dashed line. This situation can arise when either (i) $A^{\mathrm{o}}_{\mathrm{BPE}} \gg A^{\mathrm{w}}_{\mathrm{BPE}}$ and $k^0_{\mathrm{o}} \approx k^0_{\mathrm{w}}$, (ii) $A^{\mathrm{o}}_{\mathrm{BPE}}k^0_{\mathrm{o}} \approx A^{\mathrm{w}}_{\mathrm{BPE}}k^0_{\mathrm{w}}$ and $k^0_{\mathrm{o}} \gg k^0_{\mathrm{w}}$, or (iii) $A^{\mathrm{o}}_{\mathrm{BPE}} \gg A^{\mathrm{w}}_{\mathrm{BPE}}$ and $k^0_{\mathrm{o}} \gg k^0_{\mathrm{w}}$. In this scenario, the BPE undergoes capacitive charging with electrons to raise the LZO and ensure that the reduction reaction in the aqueous compartment will have a very high driving force.

Thirdly, if $A^{\mathrm{o}}_{\mathrm{BPE}}k^0_{\mathrm{o}} \ll A^{\mathrm{w}}_{\mathrm{BPE}}k^0_{\mathrm{w}}$, additional driving force is required to drive the oxidation half-reaction at the organic pole (see Eqn (5)) at the same rate as the reduction half-reaction at the aqueous pole (see Eqn (6)). At steady-state under an external bias, the LZO is positioned closer to $E^{\mathrm{w},t=x}_{\mathrm{F,\,A_w^0/A_w}^{n_w-}}$, see Scheme 4B, dashed line. This situation can arise when either (i) $A^{\mathrm{o}}_{\mathrm{BPE}} \ll A^{\mathrm{w}}_{\mathrm{BPE}}$ and $k^0_{\mathrm{o}} \approx k^0_{\mathrm{w}}$, (ii) $A^{\mathrm{o}}_{\mathrm{BPE}}k^0_{\mathrm{o}} \approx A^{\mathrm{w}}_{\mathrm{BPE}}k^0_{\mathrm{w}}$ and $k^0_{\mathrm{o}} \ll k^0_{\mathrm{w}}$, or (iii) $A^{\mathrm{o}}_{\mathrm{BPE}} \ll A^{\mathrm{w}}_{\mathrm{BPE}}$ and $k^0_{\mathrm{o}} \ll k^0_{\mathrm{w}}$. In this scenario, the BPE is completely discharged of electrons to lower LZO and ensure that the oxidation reaction in the organic compartment will have a very high driving force.

Fourthly, if $A^{\mathrm{o}}_{\mathrm{BPE}}k^0_{\mathrm{o}} \approx A^{\mathrm{w}}_{\mathrm{BPE}}k^0_{\mathrm{w}}$, the kinetics are reasonably facile, and concentration polarization is ignored, then an excess of bulk concentration of one redox species over the other significantly influences the position of LZO as the $A^{\mathrm{w}}_{\mathrm{BPE}}k^0_{\mathrm{w}}c^s_{\mathrm{A_w^0}}/A^{\mathrm{o}}_{\mathrm{BPE}}k^0_{\mathrm{o}}c^s_{\mathrm{D_o^0}}$ ratio in Eqn (17) is then solely controlled by the surface concentration ratio $c^s_{\mathrm{A_w^0}}/c^s_{\mathrm{D_o^0}}$, see Schemes 4C and D. In other words, if $c^b_{\mathrm{D_o}^{n_o+}}/c^b_{\mathrm{D_o^0}} \gg c^b_{\mathrm{A_w^0}}/c^b_{\mathrm{A_w}^{n_w-}}$, when a positive external bias is applied and the surface concentration ratios $c^s_{\mathrm{D_o}^{n_o+}}/c^s_{\mathrm{D_o^0}}$ and $c^s_{\mathrm{A_w^0}}/c^s_{\mathrm{A_w}^{n_w-}}$ adjust to the new $\Delta^{\mathrm{w}}_{\mathrm{o}}\phi_{\mathrm{eq.}}$ at the poles of the BPE in the organic and aqueous compartments, respectively, $c^s_{\mathrm{A_w^0}}$ decreases significantly whereas $c^s_{\mathrm{D_o^0}}$ remains relatively unaffected. Thus, while $E^{\mathrm{w}}_{\mathrm{F,\,A_w^0/A_w}^{n_w-}}$ shifts negatively, $E^{\mathrm{o}}_{\mathrm{F,\,D_o}^{n_o+}/\mathrm{D_o^0}}$ remains pinned close to $E^{\mathrm{o},t=0}_{\mathrm{F,\,D_o}^{n_o+}/\mathrm{D_o^0}}$. As the electron transfer reaction proceeds from $t = x$ to a steady-state at $t = \infty$ (represented by the blue arrow), $E^{\mathrm{o}}_{\mathrm{F,\,D_o}^{n_o+}/\mathrm{D_o^0}}$ continues to remain pinned and the LZO equilibrates close to $E^{\mathrm{o},t=0}_{\mathrm{F,\,D_o}^{n_o+}/\mathrm{D_o^0}}$, see Scheme 4C, dashed line. In this scenario, the organic redox couple in excess, $\mathrm{D_o}^{n_o+}/\mathrm{D_o^0}$ with $c^b_{\mathrm{D_o}^{n_o+}} \approx c^b_{\mathrm{D_o^0}}$, effectively acts as an electrode to reduce the aqueous redox couple, $\mathrm{A_w^0/A_w}^{n_w-}$, as described in Eqns (5) and (6). Now the system response becomes identical to that of a conventional three-electrode electrochemical cell, controlled by the electrochemical reaction taking place at the pole of the BPE in the aqueous compartment (Eqn (6)). Finally, if $c^b_{\mathrm{D_o}^{n_o+}}/c^b_{\mathrm{D_o^0}} \ll c^b_{\mathrm{A_w^0}}/c^b_{\mathrm{A_w}^{n_w-}}$, the LZO equilibrates close to $E^{\mathrm{w},t=0}_{\mathrm{F,\,A_w^0/A_w}^{n_w-}}$, see Scheme 4D, dashed line, and the system response is controlled by the electrochemical reaction taking place at the pole of the BPE in the organic compartment (Eqn (5)).

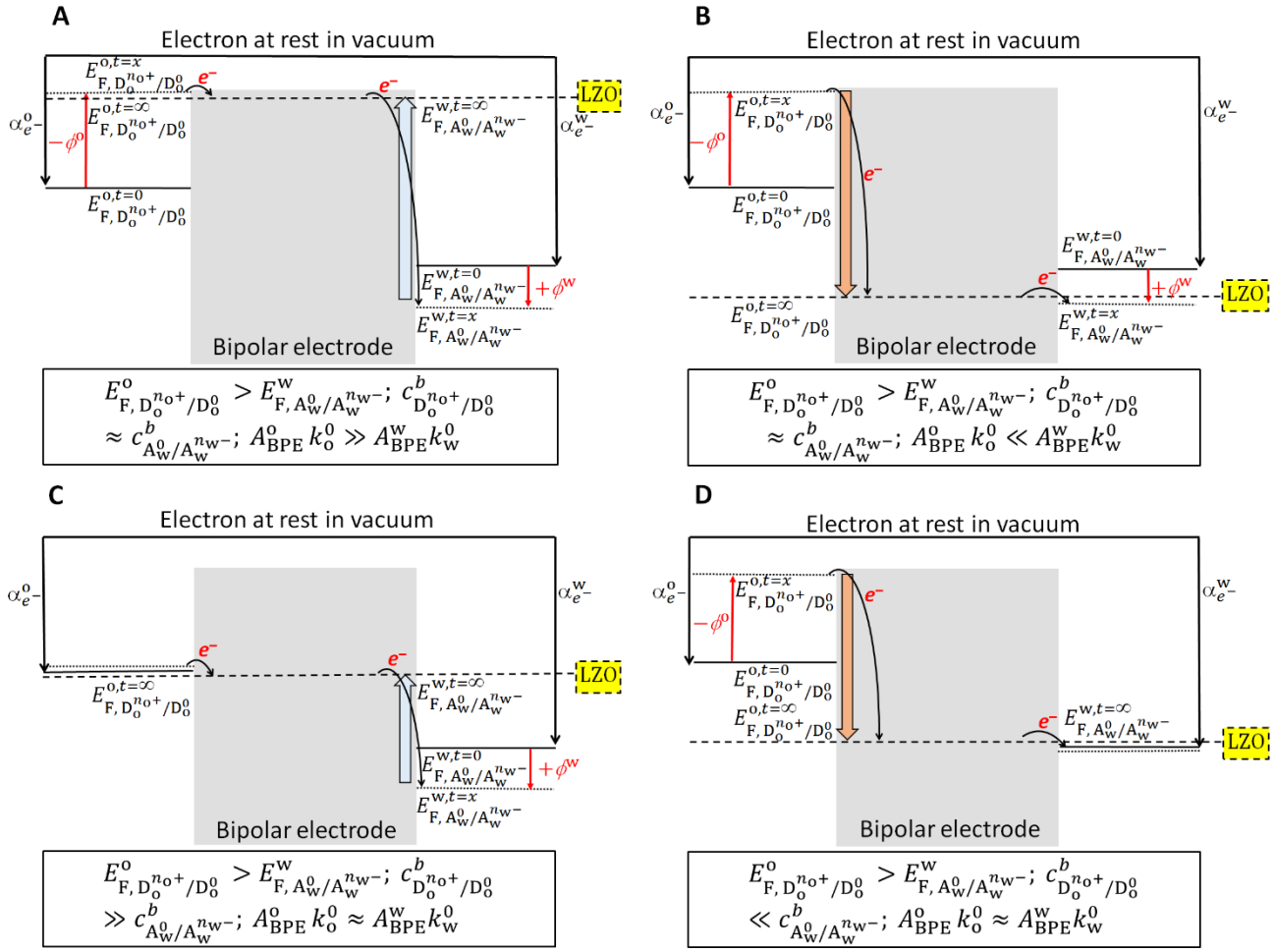

Scheme 4 Schematics comparing the effects of various experimental variables on the thermodynamics of Fermi level equilibration between electron donor and acceptor redox couples at opposite poles of the BPE for 4-electrode CBPECs with immiscible aqueous-organic electrolyte solutions under external bias and with a strong reductant in the organic phase ($E^{o,t=0}_{F,D^{n_o+}_o/D^0_o} > E^{w,t=0}_{F,A^0_w/A^{n_w-}_w}$). In all schemes, the Fermi levels of the electrons in solution prior to the application of an external bias at $t = 0$ are represented by solid black lines, whereas on application of an external bias at $t = x$ they are represented as dotted black lines. The equilibrium positions at $t = \infty$ are represented by dashed black lines. In schemes (**a, b**), no excess of either redox species is present ($c^b_{D^{n_o+}_o}/c^b_{D^0_o} \approx c^b_{A^0_w}/c^b_{A^{n_w-}_w}$) and the influence of the relationships between the area of the poles of the BPE and the potential-independent rate constants for the redox reaction in each compartment on the position of the LZO at equilibrium is highlighted with either (**a**) $A^o_{BPE}k^0_o \gg A^w_{BPE}k^0_w$ or (**b**) $A^o_{BPE}k^0_o \ll A^w_{BPE}k^0_w$ (**b**). In schemes (**c, d**), $A^o_{BPE}k^0_o \approx A^w_{BPE}k^0_w$ and the influence of an excess of a redox species in one compartment on the position of the LZO at equilibrium is highlighted with either (**c**) $c^b_{D^{n_o+}_o}/c^b_{D^0_o} \gg c^b_{A^0_w}/c^b_{A^{n_w-}_w}$ or (**d**) $c^b_{D^{n_o+}_o}/c^b_{D^0_o} \ll c^b_{A^0_w}/c^b_{A^{n_w-}_w}$.

Finally, it is worth considering what happens once a steady-state has been reached under an external bias, the LZO has been established as defined in Eqn (17), and then the biasing of the driving electrodes in each phase is switched off. During the bipolar electrochemical reaction, only the surface concentration ratios of the redox couples at each pole of the BPE are adjusted in each compartment until Fermi level equilibration was achieved (*i.e,* $E^{w}_{F,A^0_w/A^{n_w-}_w} = E^{o}_{F,D^{n_o+}_o/D^0_o}$ at the surface of the aqueous and organic poles of the BPE, respectively). Therefore, on switching off the driving electrodes, with sufficient time for the redox species in bulk to mix with the redox species at the surface of each pole of the BPE, the concentration ratios at the surface will once again match the concentrations ratios in bulk (as was the case initially at $t = 0$ before biasing the driving electrodes).

The principles and equations outlined in this section provide the conceptual and theoretical platform to perform finite element simulations modelling the observed or expected electrochemical responses for 4-electrode CBPEC systems. In particular, such simulations will be essential to derive quantitative meaning from electrochemical experiments performed with in-built asymmetries (reaction area, kinetics, redox potentials, *etc.*) influencing the redox processes at each pole of the BPE.

5. The basis of the features of a cyclic voltammogram obtained in a 4-electrode CBPEC with immiscible aqueous-organic solutions

A sample cyclic voltammogram from a 4-electrode CBPEC with immiscible aqueous-organic solutions is shown in Fig. 1. Equimolar solutions of A^0_w and D^0_o are present in the aqueous and organic compartments, as depicted in Scheme 2. Details of the experimental procedure to calibrate the raw CV data to the Galvani scale ($\Delta^w_o\phi$ / V) is beyond the extent of this perspective but has been described previously.[27,31,32] In Fig. 1, the redox

species were chosen such that $E^{o,t=0}_{F,\,D^{n_o+}_o/D^0_o} > E^{w,t=0}_{F,\,A^0_w/A^{n_w-}_w}$ based on their standard redox potentials. Thus, at t = 0, no current flows through the BPE due to the lack of a mechanism to maintain electroneutrality in each phase prior to applying an external bias, and an equilibrium Galvani potential difference ($\Delta^w_o\phi^{t=0}_{eq.}$) is established.

The observed CV in Fig. 1 may be understood using the theory outlined *vide supra*. The starting applied Galvani potential difference ($\Delta^w_o\phi$) for the CV is –0.65 V, the switching $\Delta^w_o\phi$ is +0.25 V and the final $\Delta^w_o\phi$ is –0.65 V. The scan direction is indicated by the red arrows. Initially, from –0.65 V to ca. –0.50 V no noticeable electron transfer takes place. This indicates that, at these $\Delta^w_o\phi$ values, the overpotentials for the anodic ($\eta_{an.}$) and cathodic ($\eta_{cat.}$) half-reactions at the ends of each pole of the BPE, and hence the equilibrium Galvani potential difference ($\Delta^w_o\phi^{t=x}_{eq.}$), are not sufficient to drive electron transfer between the redox couples in each compartment with significant kinetics. Only once $\Delta^w_o\phi$ is polarized more positively, at ca. –0.4 V, do we see the onset of a positive peak on the CV. At this $\Delta^w_o\phi$ value, $\Delta^w_o\phi^{t=x}_{eq.}$ is of sufficient magnitude to induce electron transfer along the BPE with appreciable kinetics, thereby establishing a new equilibria between $E^w_{F,\,A^0_w/A^{n_w-}_w}$ and $E^o_{F,\,D^{n_o+}_o/D^0_o}$ and causing the surface concentration ratios of the organic donor ($c^s_{D^{n_o+}_o}/c^s_{D^0_o}$) and aqueous acceptor ($c^s_{A^0_w}/c^s_{A^{n_w-}_w}$) redox species to adjust at the organic and aqueous poles of the BPE, respectively. When the sweep direction is reversed and scanned negatively at ca. –0.1 V, $c^s_{D^{n_o+}_o}/c^s_{D^0_o}$ and $c^s_{A^0_w}/c^s_{A^{n_w-}_w}$ adjust again and current flows from the aqueous to organic compartment giving rise to a negative peak on the CV.

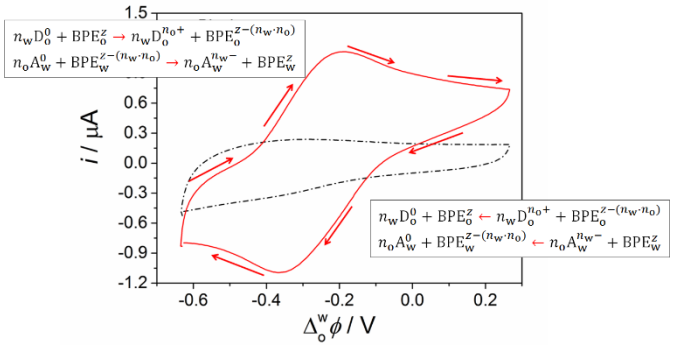

Fig. 1 Cyclic voltammograms (CV) for a 4-electrode CBPEC with immiscible aqueous-organic solutions with (red solid CV) or without (black dash-dot CV) a hydrophilic electron acceptor species (A^0_w) in the aqueous phase and a lipophilic electron donor species (D^0_o) in the organic phase. The redox species were chosen such that $E^{o,t=0}_{F,\,D^{n_o+}_o/D^0_o} > E^{w,t=0}_{F,\,A^0_w/A^{n_w-}_w}$, and neither redox species was in excess. The BPE consisted of two metallic electrodes (*e.g.,* platinum or gold electrodes are ideal), one immersed in each phase and connected by an electric wire. The BPE is chemically stable under the experimental conditions employed. The driving electrodes in each phase were platinum wires and the *pseudo*-reference electrodes were Ag/AgCl wires, one immersed in the aqueous electrolyte and the other in the organic reference solution in the organic compartment. The aqueous phase was a solution of sodium chloride and the organic phase was α,α,α-trifluorotoluene with bis(triphenylphosphoranylidene) ammonium tetrakis(pentafluorophenyl)borate as the supporting electrolyte. The scan rate was 20 mV·s^{-1}. The oxidation and reduction half-reactions occurring at the organic and aqueous poles of the BPE are described by Eqns (5) and (6), respectively. The directions of the two half-reactions giving rise to the anodic and cathodic peaks are shown in the text boxes.

Based on the CV in Fig. 1, if a chronoamperometric experiment was carried out and $\Delta^w_o\phi$ set to +0.1 V, electrons would flow from the organic to aqueous compartments, as described in Eqns (5) and (6), giving rise to a positive current. With time, $E^o_{F,\,D^{n_o+}_o/D^0_o}$ would rapidly lower and $E^w_{F,\,A^0_w/A^{n_w-}_w}$ rapidly rise, as $c^s_{D^{n_o+}_o}/c^s_{D^0_o}$ and $c^s_{A^0_w}/c^s_{A^{n_w-}_w}$ adjust, immediately decreasing the magnitude of the observed positive current. Eventually, a small positive steady-state current would be established, indicating that the Fermi level of the electrons in the BPE and the Fermi levels of the electrons in both solutions were nearly equal and the LZO on the BPE was being approached. The LZO is never actually reached, however, with a small current always flowing from the organic to aqueous compartments under external bias.

It is worth re-iterating that the peaks on the forward and reverse CV sweeps in Fig. 1 indicate the progress of two half-reactions. Thus, in a conventional 3-electrode electrochemical cell, the peak on the forward sweep with a positive current simply means the species in solution is being oxidized at this potential on the working electrode. However, in the 4-electrode CBPEC with immiscible aqueous-organic solutions, the peak on the forward sweep with a positive current indicates the flow of negative charge, *i.e.,* electrons, from the organic to aqueous compartment with concomitant reduction of A^0_w to $A^{n_w-}_w$ and oxidation of D^0_o to $D^{n_o+}_o$, as outlined in Eqns (5) and (6). When the sweep direction is reversed and scanned negatively, at ca. –0.1 V the back-reactions of Eqns (5) and (6) take place and now negative charge flows from the aqueous to organic compartment producing the peak on the reverse sweep with a negative current.

6. Conclusions

Herein, we have summarized the current state-of-the-art in the emerging fields of open and closed bipolar electrochemistry in a 4-electrode configuration with a focus on immiscible aqueous-organic electrolyte solutions. We have presented theory based on Fermi level equilibration between redox species in separate immiscible solutions, both in contact with opposite poles of a bipolar electrode and subject to an external bias, to understand the thermodynamics underpinning the technique of closed bipolar electrochemistry in a 4-electrode configuration with immiscible aqueous-organic electrolyte solutions. In particular, we have focused on the concept of the Line of Zero Overpotential (LZO) on the bipolar electrode, which is equivalent to the Fermi level of the bipolar electrode at steady-state conditions under an external bias ($E^{t=\infty}_{F,BPE}$). In particular, we outlined the various experimental conditions, such as an excess of a redox species in one compartment over the other, different kinetics for the redox reactions taking place at each pole of the bipolar electrode, and the area of the poles of the bipolar electrode in contact with each electrolyte solution, on the final position of the LZO. This theory will provide the framework for understanding all future applications of closed bipolar electrochemistry in a 4-electrode configuration with immiscible aqueous-organic electrolyte solutions to spectro-electroanalysis, energy storage, electrocatalysis, photo-electrodechemistry, and electrodeposition. Furthermore, the theory presented herein is equally applicable to an all-aqueous based closed bipolar electrochemical cell in a 4-electrode configuration, *i.e.,* two compartments with aqueous electrolyte

solutions containing redox active species and connected by a bipolar electrode.

Glossary of abbreviations and symbols

AVS = absolute vacuum scale.

A_w^0 (or $A_w^{n_w-}$) = oxidized (or reduced) form of the aqueous electron acceptor.

A_{BPE}^w (or A_{BPE}^o) = area of the pole of the bipolar electrode in the aqueous (or organic) compartment undergoing an electrochemical half-reaction.

BPE = bipolar electrode.

CBPEC = closed bipolar electrochemical cell.

$c_{A_w^0}^b/c_{A_w^{n_w-}}^b$ (or $c_{D_o^{n_o+}}^b/c_{D_o^0}^b$) = ratio of the bulk concentrations of the aqueous (or organic) redox species.

$c_{A_w^0}^s/c_{A_w^{n_w-}}^s$ (or $c_{D_o^{n_o+}}^s/c_{D_o^0}^s$) = ratio of the surface concentrations of the aqueous (or organic) redox species.

α_w (or α_o) = charge transfer coefficient in the aqueous (or organic) phase.

D_o^0 (or $D_o^{n_o+}$) = oxidized (or reduced) form of the organic electron donor.

e = the elementary charge.

ECSOW = electron conductor separating oil-water.

ECL = electrochemiluminescence.

$E_{F,Ox/Red}^S$ = Fermi level of a redox couple in solution S.

$E_{F,BPE}$ = Fermi level of the bipolar electrode.

$E_{F,A_w^0/A_w^{n_w-}}^w$ (or $E_{F,D_o^{n_o+}/D_o^0}^o$) = Fermi level of the electrons in the aqueous (or organic) redox couple.

$[Fe^{(III)}(CN)_6]^{3-}/Fe^{(II)}(CN)_6]^{4-}$ = ferri-/ferrocyanide redox couple

F= Faraday's constant.

Fc^+/Fc = ferrocenium cation/ferrocene redox couple.

ϕ^S = Galvani (inner) potential of solution S.

$\Delta_o^w\phi$ = Galvani potential difference between the aqueous (w) and organic (o) solutions.

$\Delta_o^w\phi_{eq.}$ = equilibrium Galvani potential difference.

$\Delta_o^w\phi_{HET}^{\ominus}$ = standard Galvani potential difference for the heterogeneous electron transfer.

$\Delta G_{Red}^{\ominus}$ = standard Gibbs energy of reduction.

HET = heterogeneous electron transfer.

i_{BPE}^w (or i_{BPE}^o) = current for the half-reaction at the pole of the bipolar electrode in the aqueous (or organic) compartment.

k_w^0 (or k_o^0) = potential-independent rate constant at the aqueous (or organic) pole of the bipolar electrode.

ITIES = interface between two immiscible electrolyte solutions.

LZO = line of zero overpotential.

N_a = Avogadro's constant.

NP = nanoparticle.

n_w (or n_o) = number of electrons exchanged for the aqueous (or organic) redox couple.

OBPEC= open bipolar electrochemical cell.

Ox/Red = oxidized/reduced redox couple.

$\left[E_{H^+/{}^1/_2H_2}^{\ominus}\right]_{AVS}^w$ = potential of the standard hydrogen electrode on the absolute vacuum scale.

$\left[E_{Ox/Red}^{\ominus}\right]_{AVS}^S$ = standard redox potential of the redox reaction.

$\left[E_{A_w^0/A_w^{n_w-}}^{\ominus}\right]_{SHE}^w$ (or $\left[E_{D_o^{n_o+}/D_o^0}^{\ominus}\right]_{SHE}^o$)= standard redox potential of the aqueous electron acceptor (or organic electron donor).

$\tilde{\mu}_{e^-}^S$ = electrochemical potential of an electron in Ox/Red in solution S.

$\tilde{\mu}_{Ox}^S$ (or $\tilde{\mu}_{Red}^S$) = electrochemical potential of oxidation (or reduction) in solution S.

$\mu_{Ox}^{\ominus,S}$ (or $\mu_{Red}^{\ominus,S}$) = standard chemical potential of oxidation (or reduction) in solution S.

$\alpha_{e^-}^S$ = real chemical potential of an electron in Ox/Red in solution S.

ψ^S = outer potential of solution S.

χ^S = surface potential of solution S.

SHE = standard hydrogen electrode.

SWCNT = single-walled carbon nanotube.

$\eta_{cat.}$ (or $\eta_{an.}$) = overpotential, *i.e,* driving force, for the cathodic reduction (or anodic oxidation) reaction.

Φ^S = work function of solution S.

z = charge on poles of the bipolar electrode.

Acknowledgements

This publication has emanated from research by M.D.S. and A.F.M.-O. supported by the European Research Council through a Starting Grant (agreement no.716792) and in part by a research grant from Science Foundation Ireland (SFI) (grant number 13/SIRG/2137). A.G.-Q. acknowledges funding received from an Irish Research Council Government of Ireland Postdoctoral Fellowship Award (grant number GOIPD/2018/252). P.P. gratefully acknowledges the Academy Research Fellow funding from the Academy of Finland (Grant number 315739).

Conflicts of interest

There are no conflicts to declare.

Notes and references

1 F. Mavré, R. K. Anand, D. R. Laws, K. F. Chow, B. Y. Chang, J. A. Crooks and R. M. Crooks, *Anal. Chem.*, 2010, **82**, 8766–8774.

2 J. Duval, J. M. Kleijn and H. P. Van Leeuwen, *J. Electroanal. Chem.*, 2001, **505**, 1–11.

3 M. Li, S. Liu, Y. Jiang and W. Wang, *Anal. Chem.*, 2018, **90**, 6390–6396.

4 X. Zhang, J. Li, X. Jia, D. Li and E. Wang, *Anal. Chem.*, 2014, **86**, 5595–5599.

5 S. Wu, Z. Zhou, L. Xu, B. Su and Q. Fang, *Biosens. Bioelectron.*, 2014, **53**, 148–153.

6 A. de Poulpiquet, B. Diez-Buitrago, M. Milutinovic, B. Goudeau, L. Bouffier, S. Arbault, A. Kuhn and N. Sojic, *ChemElectroChem*, 2016, **3**, 404–409.

7 S. Goodwin and D. A. Walsh, *ACS Appl. Mater. Interfaces*, 2017, **9**, 23654–23661.
8 H. Wu and K. Lian, *J. Power Sources*, 2018, **378**, 209–215.
9 A. Allagui, J. M. Ashraf, M. Khalil, M. A. Abdelkareem, A. S. Elwakil and H. Alawadhi, *ChemElectroChem*, 2017, **4**, 2084–2090.
10 S. E. Fosdick and R. M. Crooks, *J. Am. Chem. Soc.*, 2012, **134**, 863–866.
11 S. E. Fosdick, S. P. Berglund, C. B. Mullins and R. M. Crooks, *Anal. Chem.*, 2013, **85**, 2493–2499.
12 S. E. Fosdick, S. P. Berglund, C. B. Mullins and R. M. Crooks, *ACS Catal.*, 2014, **4**, 1332–1339.
13 C. Kumsapaya, M.-F. Bakaï, G. Loget, B. Goudeau, C. Warakulwit, J. Limtrakul, A. Kuhn and D. Zigah, *Chem. - A Eur. J.*, 2013, **19**, 1577–1580.
14 C. Kumsapaya, J. Limtrakul, A. Kuhn, D. Zigah and C. Warakulwit, *ChemElectroChem*, 2016, **3**, 410–414.
15 L. Koefoed, S. U. Pedersen and K. Daasbjerg, *ChemElectroChem*, 2016, **3**, 495–501.
16 G. Loget, J. Roche, E. Gianessi, L. Bouffier and A. Kuhn, *J. Am. Chem. Soc.*, 2012, **134**, 20033–20036.
17 Y. Koizumi, N. Shida, M. Ohira, H. Nishiyama, I. Tomita and S. Inagi, *Nat. Commun.*, 2016, **7**, 1–6.
18 G. Tisserant, Z. Fattah, C. Ayela, J. Roche, B. Plano, D. Zigah, B. Goudeau, A. Kuhn and L. Bouffier, *Electrochim. Acta*, 2015, **179**, 276–281.
19 G. Loget, D. Zigah, L. Bouffier, N. Sojic and A. Kuhn, *Acc. Chem. Res.*, 2013, **46**, 2513–2523.
20 D. Plana, F. G. E. Jones and R. A. W. Dryfe, *J. Electroanal. Chem.*, 2010, **646**, 107–113.
21 D. Plana, G. Shul, M. J. Stephenson and R. A. W. Dryfe, *Electrochem. commun.*, 2009, **11**, 61–64.
22 J. P. Guerrette, S. M. Oja and B. Zhang, *Anal. Chem.*, 2012, **84**, 1609–1616.
23 J. T. Cox, J. P. Guerrette and B. Zhang, *Anal. Chem.*, 2012, **84**, 8797–8804.
24 V. Eßmann, F. Zhao, V. Hartmann, M. M. Nowaczyk, W. Schuhmann and F. Conzuelo, *Anal. Chem.*, 2017, **89**, 7160–7165.
25 W. Xu, K. Fu and P. W. Bohn, *ACS Sensors*, 2017, **2**, 1020–1026.
26 M. Ongaro, A. Gambirasi, M. Favaro, A. Kuhn and P. Ugo, *Electrochim. Acta*, 2014, **116**, 421–428.
27 H. Hotta, N. Akagi, T. Sugihara, S. Ichikawa and T. Osakai, *Electrochem. commun.*, 2002, **4**, 472–477.
28 P. Vanýsek and L. B. Ramírez, *J. Chil. Chem. Soc.*, 2008, **53**, 1455–1463.
29 E. Smirnov, P. Peljo, M. D. Scanlon and H. H. Girault, *ACS Nano*, 2015, **9**, 6565–6575.
30 M. D. Scanlon, P. Peljo, M. A. Méndez, E. Smirnov and H. H. Girault, *Chem. Sci.*, 2015, **6**, 2705–2720.
31 E. Smirnov, P. Peljo, M. D. Scanlon and H. H. Girault, *Electrochim. Acta*, 2016, **197**, 362–373.
32 Y. Gründer, M. D. Fabian, S. G. Booth, D. Plana, D. J. Fermín, P. I. Hill and R. A. W. Dryfe, *Electrochim. Acta*, 2013, **110**, 809–815.
33 P. S. Toth, Q. M. Ramasse, M. Velický and R. A. W. Dryfe, *Chem. Sci.*, 2015, **6**, 1316–1323.
34 P. S. Toth, A. K. Rabiu and R. A. W. Dryfe, *Electrochem. commun.*, 2015, **60**, 153–157.
35 S. Rastgar, H. Deng, F. Cortés-Salazar, M. D. Scanlon, M. Pribil, V. Amstutz, A. A. Karyakin, S. Shahrokhian and H. H. Girault, *ChemElectroChem*, 2014, **1**, 59–63.
36 M. D. Scanlon, P. Peljo, L. Rivier, H Vrubel and H. H. Girault, *Phys. Chem. Chem. Phys.*, 2017, **19**, 22700–22710.
37 J. J. Nieminen, I. Hatay, P. Ge, M. A. Méndez, L. Murtomäki and H. H. Girault, *Chem. Commun.*, 2011, **47**, 5548–5550.
38 M. D. Scanlon, X. Bian, H. Vrubel, V. Amstutz, K. Schenk, X. Hu, B. Liu and H. H. Girault, *Phys. Chem. Chem. Phys.*, 2013, **15**, 2847–57.
39 M. D. Scanlon, E. Smirnov, T. J. Stockmann and P. Peljo, *Chem. Rev.*, 2018, **118**, 3722–3751.
40 P. Peljo, M. D. Scanlon, A. J. Olaya, L. Rivier, E. Smirnov and H. H. Girault, *J. Phys. Chem. Lett.*, 2017, **8**, 3564–3575.
41 A. N. J. Rodgers and R. A. W. Dryfe, *ChemElectroChem*, 2016, **3**, 472–479.
42 P. Ge, M. D. Scanlon, P. Peljo, X. Bian, H. Vubrel, A. O'Neill, J. N. Coleman, M. Cantoni, X. Hu, K. Kontturi, B. Liu and H. H. Girault, *Chem. Commun.*, 2012, **48**, 6484–6486.
43 X. Bian, M. D. Scanlon, S. Wang, L. Liao, Y. Tang, B. Liu and H. H. Girault, *Chem. Sci.*, 2013, **4**, 3432–3441.
44 T. J. Stockmann, L. Angelé, V. Brasiliense, C. Combellas and F. Kanoufi, *Angew. Chemie Int. Ed.*, 2017, **56**, 13493–13497.
45 A. Uehara, T. Hashimoto and R. A. W. Dryfe, *Electrochim. Acta*, 2014, **118**, 26–32.
46 Y. Zhang, N. Nishi, K. ichi Amano and T. Sakka, *Electrochim. Acta*, 2018, **282**, 886–891.
47 N. Nishi, T. Kakinami and T. Sakka, *Chem. Commun.*, 2015, **51**, 13638–13641.
48 H. Hotta, S. Ichikawa, T. Sugihara and T. Osakai, *J. Phys. Chem. B*, 2003, **107**, 9717–9725.
49 P. Peljo, E. Smirnov and H. H. Girault, *J. Electroanal. Chem.*, 2016, **779**, 187–198.
50 S. E. Fosdick, K. N. Knust, K. Scida and R. M. Crooks, *Angew. Chemie - Int. Ed.*, 2013, **52**, 10438–10456.
51 S. M. Khoshfetrat, H. Bagheri and M. A. Mehrgardi, *Biosens. Bioelectron.*, 2018, **100**, 382–388.
52 S. Ge, J. Zhao, S. Wang, F. Lan, M. Yan and J. Yu, *Biosens. Bioelectron.*, 2018, **102**, 411–417.
53 H. J. Lu, W. Zhao, J. J. Xu and H. Y. Chen, *Biosens. Bioelectron.*, 2018, **102**, 624–630.
54 Q. Zhai, X. Zhang, Y. Xia, J. Li and E. Wang, *Analyst*, 2016, **141**, 3985–3988.
55 X. Zhang, L. Zhang, Q. Zhai, W. Gu, J. Li and E. Wang, *Anal. Chem.*, 2016, **88**, 2543–2547.
56 X. Yu, J. Liang, T. Yang, M. Gong, D. Xi and H. Liu, *Biosens. Bioelectron.*, 2018, **99**, 163–169.
57 H. Xing, X. Zhang, Q. Zhai, J. Li and E. Wang, *Anal. Chem.*, 2017, **89**, 3867–3872.
58 J. P. Guerrette, S. J. Percival and B. Zhang, *J. Am. Chem. Soc.*, 2013, **135**, 855–861.
59 Y. Fan, R. Hao, C. Han and B. Zhang, *Anal. Chem.*, 2018, **90**, 13837–13841.

60 R. Hao, Y. Fan, C. Han and B. Zhang, *Anal. Chem.*, 2017, **89**, 12652–12658.

61 Q. Zhai, X. Zhang, Y. Han, J. Zhai, J. Li and E. Wang, *Anal. Chem.*, 2016, **88**, 945–951.

62 D. Ibañez, A. Heras and A. Colina, *Anal. Chem.*, 2017, **89**, 3879–3883.

63 D. J. Fermin and N. Eugster, in *N4-Macrocyclic Metal Complexes*, eds. J. H. Zagal, F. Bedioui and J.-P. Dodelet, Springer Science+Business Media, Inc., New York, 2006, pp. 517–574.

64 D. J. Fermín, Z. Ding, H. D. Duong, P.-F. Brevet and H. H. Girault, *J. Phys. Chem. B*, 1998, **102**, 10334–10341.

65 D. J. Fermín, H. D. Duong, Z. Ding, P. F. Brevet and H. H. Girault, *J. Am. Chem. Soc.*, 1999, **121**, 10203–10210.

66 H. Jensen, J. J. Kakkassery, H. Nagatani, D. J. Fermín and H. H. Girault, *J. Am. Chem. Soc.*, 2000, **122**, 10943–10948.

67 N. Eugster, H. Jensen, D. J. Fermín and H. H. Girault, *J. Electroanal. Chem.*, 2003, **560**, 143–149.

68 D. Plana, K. A. Bradley, D. Tiwari and D. J. Fermín, *Phys. Chem. Chem. Phys.*, 2016, **18**, 12428–12433.

69 D. Plana and D. J. Fermín, *J. Electroanal. Chem.*, 2016, **780**, 373–378.

70 B. Su, D. J. Fermín, J.-P. Abid, N. Eugster and H. H. Girault, *J. Electroanal. Chem.*, 2005, **583**, 241–247.

71 D. J. Fermin, H. Jensen, J. E. Moser and H. H. Girault, *ChemPhysChem*, 2003, **4**, 85–89.

72 J. K. Cooper and I. Benjamin, *J. Phys. Chem. B*, 2014, **118**, 7703–7714.

73 P. S. Toth, A. N. J. Rodgers, A. K. Rabiu, D. Ibañez, J. X. Yang, A. Colina and R. A. W. Dryfe, *J. Mater. Chem. A*, 2016, **4**, 7365–7371.

